

Extracting Information from the Gravitational Redshift of Compact Rotating Objects

Paul Nunez

Department of Physics,
University of Utah,
115 S 1400 E, Salt Lake City, UT 84112
and

Observatorio Astronómico,
Universidad Sergio Arboleda,
C.L. 74 No. 14-14, Bogota, Colombia

Marek Nowakowski

Departamento de Física, Universidad de los Andes,
Cra. 1E No. 18A-10, Bogota, Colombia.

February 21, 2024

Abstract

When rotation is not taken into account, the measurement of the Gravitational Redshift can provide unique information about the compactness (M/R) of the star. Rotation alters the gravitational redshift rendering thereby a unique determination of the compactness parameter impossible. Nevertheless, it can be shown that by using some theoretical input, useful information on, say, the radii of compact rotating objects can still be extracted. Moreover, by measuring the gravitational redshift one can infer the maximum angular velocity of the object. As it is well known, the minimum observed periods of rotation are found in millisecond pulsars. Here we show that millisecond periods are actually a semi-theoretical limit that can be found by General Relativistic arguments corresponding to the maximum angular velocity. We apply our method to compact objects such as pulsars, white dwarfs and neutron stars.

Keywords: maximum angular velocity; stars: neutron; stars: rotation
PACS: 04.40.Dg, 97.60.Jd

1 Introduction

Compact Objects such as neutron stars [1, 2] have radii very close to their Schwarzschild radii and hence General Relativity should be used to describe the gravity close to their surface. Neglecting rotation, the geometry of space-time can be described using the well

known spherically symmetric Schwarzschild geometry and information on the ratio M/R of a compact object can be obtained from the (observed) gravitational redshift ([3], [4]). This is a useful, model-independent way, to gain insight into properties of neutron stars and white dwarfs. Although it is a model-independent procedure, it relies on certain basic assumptions, like the absence of rotation and a perfect spherical symmetry (i.e. zero quadrupole moment). To gain a deeper understanding it makes then sense to relax some of these assumptions and to examine what information can be extracted from the gravitational redshift in the more general case. In the present paper, we shall study the situation with a non-zero angular velocity, but assuming that the object is rigid enough to allow the approximation of a negligible quadrupole moment. In particular, when rotation is taken into account, spherical symmetry is lost and off-diagonal terms appear in the metric which has the following general form :

$$ds^2 = g_{tt}dt^2 + g_{rr}dr^2 + g_{\theta\theta}d\theta^2 + g_{\phi\phi}d\phi^2 + 2g_{t\phi}dt d\phi: \quad (1)$$

The exact form of this metric including magnetic field, quadrupole moment and even radiation ([5], [6], [7]) is still a subject of research. We will use a first and second order approximation to this metric neglecting the effects of the quadrupole moment and the magnetic field. Furthermore, it is expected that only relatively young Neutron Stars can have a differential rotation [1] (encountered also in boson stars [8]) which we therefore neglect here.

Deriving the gravitational redshift from (1) we will show that, for a fixed mass, a unique solution for the radius of the compact object does not exist. Instead, we obtain two different solutions which can differ by orders of magnitude as long as the angular velocity is not too large. In this case, all theoretical models still favor the solution of the smaller radius and we can select this solution without the necessity to refer to some details of a specific model. With increasing angular momentum, the two radii approach each other and the above selection rule is not effective anymore. However, in such a case we can define a narrow range of allowed radii which is still a valuable model independent information for fast rotating objects.

As a bonus of our examination of the properties of the gravitational redshift Z , we can show that there exists an upper bound on the angular velocity depending on the redshift. One can even put an absolute upper bound which is independent of Z . Interestingly the bounds come out to be in the range of the observed millisecond pulsars. This in turn allows us to assume that the angular velocity of millisecond pulsars is indeed approaching its maximal value. The consequences of this assumption will be discussed in the text below. One of them is the confirmation of the result that the light emitted in very fast millisecond pulsars stems mostly from the equatorial region ([9], [10], [11]). We compare our results to the so called 'Mass Shedding Limit' [12] and to other work related to the maximum angular velocity.

One of the main results of the paper, discussed in section four, is that our analytical formula on maximal angular velocity is comparable to results obtained by using extensive numerical calculations. In particular, we agree with the numerical findings of reference

[13].

The essential parameters which enter our equations are the radius R , the angular velocity Ω and the mass M . The minimum central density at which a neutron star is stable is simply the density at which neutrons become unstable to beta decay ($\rho_0 \approx 8 \times 10^8 \text{ g/cm}^3$ [14]). Using the well known Oppenheimer-Volkov [15] equations and a plausible equation of state, one can construct a stellar model which provides the minimum mass of the neutron star to be around $0.08M_\odot$ which is a bit unrealistic taking into account that neutron stars are remnants of supernova explosions [16]. A more realistic value for the minimum mass is of the order of $M_{NS}^{\text{min}} \approx 1M_\odot$ [17], which is actually closer the maximum mass of a white dwarf ($1.44M_\odot$). The maximum mass of a neutron star can be found from causality arguments [18], by recalling that the speed of sound in dense matter has to be less than the speed of light ($\frac{dp}{d\rho} < c$). This condition gives a maximum mass of $M_{NS}^{\text{max}} \approx 3M_\odot$. The radii corresponding to the maximum and minimum masses can be found using the Oppenheimer-Volkov equation. Assuming an equation of state for a degenerate neutron fluid, the corresponding radii for the two extreme masses lie in the range 10 km to 100 km . This radius range can of course change if one uses a more sophisticated equation of state, subject of current controversy [17], but the orders of magnitude remain the same [19]. The canonical neutron star mass and radius are thought to be $1.4M_\odot$ and 10 km . A useful observational quantity, which agrees in order of magnitude with theoretical predictions, is the mean "measured" mass of the neutron stars in a Gaussian ensemble [20], namely

$$M_{NS} = (1.35 \pm 0.05)M_\odot \quad (2)$$

This value will be used if no other information on the masses is available.

The paper is organized as follows. In the second section we will briefly discuss the gravitational redshift as emerging from a perturbative axial symmetric metric. In section three we will use these results to determine the radius or the range of the radii of the compact object. Section four is devoted to the maximal angular velocity derived within our approach. In section five we discuss some improvements by taking into account more terms in the expansion of the metric. In section six we apply our results to some chosen compact objects like a white dwarf and neutron stars. Finally, in section seven we present our conclusions.

2 The Gravitational Redshift in a Perturbation Approach

A far away observer can measure a pulsar's angular velocity Ω , given by

$$\Omega = \frac{d\phi}{dt} = \frac{d}{d} \frac{d\phi}{dt} = \frac{u_\phi}{u^t} \quad (3)$$

Using (3), the four velocity of a stationary point on the surface can be written as

$$u^\mu = (u^t; 0; 0; 0) \quad (4)$$

Through the normalization condition of the four velocity ($u^\mu u_\mu = -1$), we obtain the time-like component of the four velocity in terms of the metric (1) and angular velocity :

$$u^t = \frac{1}{\sqrt{-g_{tt} - 2g_{t\phi} - g_{\phi\phi}\Omega^2}} : \quad (5)$$

The redshift factor can be calculated simply by recalling that the energy of radial photon ($h = c = 1$) is simply [21]

$$\begin{aligned} \epsilon &= -u^\mu \frac{dx_\mu}{d\lambda} = u^t \left(g_{tt} \frac{dt}{d\lambda} + g_{t\phi} \frac{d\phi}{d\lambda} \right) + u^\phi \left(g_{\phi t} \frac{dt}{d\lambda} + g_{\phi\phi} \frac{d\phi}{d\lambda} \right) \\ &= -u^t E + u^\phi L = u^t (E - L) \end{aligned} \quad (6)$$

with an additional parameter and E and L conserved quantities due to the existence of two killing vectors. As a consequence we can write for ϵ

$$\epsilon = \frac{E - L}{\sqrt{-g_{tt} - 2g_{t\phi} - g_{\phi\phi}\Omega^2}} ; \quad (7)$$

and the energy perceived by a distant observer ϵ_∞ can be now expressed through

$$\epsilon_\infty = Z \epsilon ; \quad (8)$$

where ϵ_∞ is the energy at the surface and Z is the redshift factor. Explicitly, the latter is given by [22]

$$Z = \frac{1}{\sqrt{-g_{tt} - 2g_{t\phi} - g_{\phi\phi}\Omega^2}} ; \quad (9)$$

This redshift can actually be measured for many objects [24]. Indeed, at the end of the paper we will employ the results of such observations. The behavior of Z as a function of the radius R for a fixed mass is displayed in figure 1a.

The calculation of Z can be made more concrete when we consider the metric (1). To a first approximation, Zeldovich and Novikov [27] apply small perturbations to the Schwarzschild geometry. The elements of the metric (1) can be calculated to be [27]

$$g_{tt} = -1 - \frac{2GM}{Rc^2} ; g_{t\phi} = \frac{2GJ \sin^2 \theta}{Rc^4} ; g_{\phi\phi} = \frac{R^2 \sin^2 \theta}{c^2} : \quad (10)$$

Here, the condition for slow rotation is given by $J \ll M R_g c$ (R_g being the Schwarzschild radius) [27]. Equation (10) allows us to calculate Z explicitly. One obtains

$$Z(M; R; J) = \frac{1}{\sqrt{-1 - \frac{2GM}{c^2 R} - \frac{4GJ \sin^2 \theta}{c^4 R} - \frac{R^2 \sin^2 \theta}{c^2} \Omega^2}} ; \quad (11)$$

Throughout the paper we will be using the Newtonian approximation for the angular momentum, ($J = \frac{2}{5} M R^2 \Omega$) [28]. In view of the results obtained in [29], this is a well-based assumption violated only for extremely high angular velocities (which are not exceeded here). Taking this into account, equation (11) simplifies to

$$Z(M; R; \Omega) = \frac{1}{\sqrt{-1 - \frac{2GM}{c^2 R} - \frac{4}{5} \frac{M R^2 \Omega^2}{c^2}}} ; \quad (12)$$

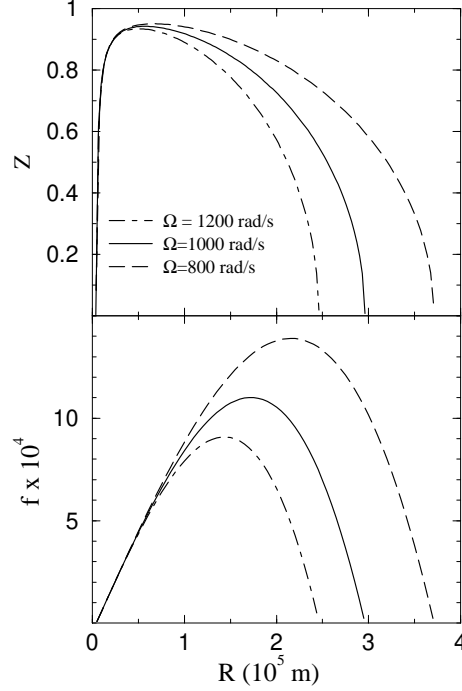


Figure 1: The top figure 'a', shows the behavior of the redshift equations (12) as a function of the radius for different angular velocities. The bottom figure 'b' shows the behavior of the corresponding polynomial (15) in units of meters. In both figures $M = 1.44M_{\odot}$. Note how the gap between the two solutions becomes narrow with increasing angular velocity.

where α , β and γ are constants given by

$$\alpha = \frac{2G}{c^2}; \quad \beta = \frac{8G}{5c^4}; \quad \gamma = \frac{1}{c^2} \quad (13)$$

and we have absorbed $\sin \theta$ into the angular momentum by defining

$$J = J_0 \sin \theta \quad (14)$$

The equations (9, 13, 14) can be now used to either solve them for the radius by assuming a mean mass or a mass range and a measured angular velocity or, alternatively to predict the redshift. Both ways will be used below.

3 Determination of the Radius

It is possible to take two different approaches when using equation (12). The first one is to demand that the term inside the parenthesis of (12) should be greater than zero, such

that after factoring out $1 - \frac{p}{R}$ one arrives at

$$f(0; R; M; \gamma) = R - M - M R^2 - R^3 = 0; \quad (15)$$

The limiting values of R correspond to the equal sign in the above equation. Since this does not depend on Z , these values have an absolute character in the sense that they give the maximal and minimal radius for any compact object with mass M and angular velocity γ regardless of the value of Z . Similar reasoning applies to any other quantity derived from (15) (e.g. r_{max}^0 in the next section).

The behavior of the function $f(0; R; M; \gamma)$ versus R is shown in figure 1b. The figure displays the global properties of this function (which can be also inferred easily analytically), like the local maximum and the two zeros, one of them close to the Schwarzschild radius.

On the other hand, we can solve the following cubic equation for the radii

$$f(Z; R; M; \gamma) = (1 - Z^2)R - M - M R^2 - R^3 = 0 \quad (16)$$

Obviously, this is the same equation as (15) if we put Z to zero in (16). Hence, we can continue examining equation (16) and discuss the absolute limits by putting $Z = 0$ at the end. The function f with non-zero gravitational redshift has the same global properties as (15). The solutions of (16) can be obtained analytically by parameterizing the Cardano formulae [30]. By a simple transformation one can get rid of the quadratic term in the cubic equation arriving at $y^3 + py + q = 0$. Depending on the sign of the discriminant $D = \left(\frac{q}{2}\right)^3 + \left(\frac{p}{3}\right)^2$, one can parameterize the solution using the auxiliary variable $F = \text{sgn}(q) \sqrt[3]{-p/3}$. In our case $D < 0$ and we parameterize the solutions through the angle ϕ given by $\cos \phi = \frac{q}{2F^3}$. The analytical solutions are then

$$r_1 = A \cos \frac{2}{3} + \frac{1}{3} \cos^{-1} \quad (17)$$

$$r_2 = A \cos \frac{4}{3} + \frac{1}{3} \cos^{-1} ; \quad (18)$$

where

$$\frac{M}{3}; A = \frac{2}{3} \sqrt{\frac{M^2}{2} + \frac{3}{2}}; \quad (19)$$

and

$$\frac{27 \frac{1024}{3375} \frac{GM}{c^3}^3 + 2 \frac{GM}{c^3} + \frac{8(1 - Z^2) GM}{15 c^3}}{2 \frac{64}{25} \frac{GM}{c^3}^2 + 3(1 - Z^2)}; \quad (20)$$

In figure 2b we have plotted r_1 and r_2 versus the angular velocity γ . The upper branch of each curve corresponds to the bigger radius meeting the lower value at some γ (this will be discussed in the next section in more detail). With growing γ the difference r between the two solutions becomes smaller, however, at relative small angular velocity

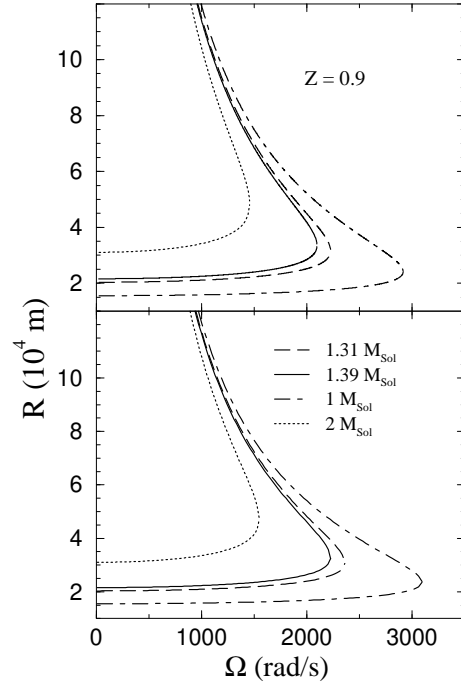


Figure 2: In these figures we show the behavior of the two solutions r_1 and r_2 as a function of the angular velocity for different masses. The top figure a' corresponds to the numerical solutions using the extended metric (33), while the bottom figure b' corresponds to the analytical solutions (17, 18). Note how the solutions meet at a particular angular velocity for each mass.

we can opt safely for the lower value of the obtained radius (close to the Schwarzschild radius) as this is favored by models. Such a point of view is not possible anymore with increasing β . Note also that the solutions $r_{1,2}$ do not determine a "range" for the radius in the strict sense. However, since both solutions depend on the mass, a range in the mass will determine a range for each of the two solutions. With this in mind, we can define a narrow range for the radius which will be explained below.

A plausible range for the mass can be given by the close extremes in the Gaussian distribution (2) as discussed in the introduction. For every limiting mass we will get a curve like in figure 2, say C_1 for the lower mass and C_2 for the upper value. The curves with an in-between mass will fill the space between the curves C_1 and C_2 . A vertical tangent to the cusp [31] of C_1 will intersect the curve C_2 in two points, r_{01} and r_{02} , which we can take as a definition of range of allowed radii. The result is a single narrow range which becomes smaller with increasing angular velocity and is zero at a maximum β . For instance, in the case of the neutron star PSR B1937+21, $r_{01} = 17600\text{m}$ and $r_{02} = 25800\text{m}$ such that $r = 8200\text{m}$. The existence of the maximum angular velocity corresponding to the cups of every curve allows even to sharpen this concept to be discussed in the next section.

It is of some interest to expand these solutions (r_1 and r_2) neglecting small terms [32] in A and β . The relevant quantities can now be approximated as

$$\frac{8GM}{15c^2}; A = \frac{2c}{3} \frac{1 - \beta^2}{\beta}; \quad (21)$$

and

$$\frac{3}{c^3} \frac{GM}{(1 - \beta^2)^{3/2}} + \frac{4}{5c^3} \frac{GM}{\beta} \frac{1 - \beta^2}{\beta} \quad (22)$$

When $\beta \rightarrow 0$, one can express r_1 and r_2 as

$$r_1 = A \frac{\beta^3}{2} - \frac{\beta^2}{6} - \frac{\beta^2}{12} \frac{1}{\beta} \quad (23)$$

$$r_2 = \frac{4}{3} + A \frac{4}{3} + \frac{4}{81} \beta^3; \quad (24)$$

The final results of our approximation reads

$$r_1 = \frac{c}{\beta} \frac{1 - \beta^2}{\beta} - \frac{GM}{c^2 (1 - \beta^2)} - \frac{12GM}{15c^2} - \frac{G^2 M^2 (4\beta^2 - 19)^2}{150c^5 (1 - \beta^2)^{5/2}} \quad (25)$$

$$r_2 = \frac{2GM}{c^2 (1 - \beta^2)} + \frac{8G^3 M^3 (19 - 4\beta^2)^3}{3375c^8 (1 - \beta^2)^4} \quad (26)$$

Note that the first term in r_2 is the Schwarzschild radius modified by a factor of $1/(1 - \beta^2)$. Actually, this term is the same result one would obtain by using a Spherically symmetric metric with no rotation.

It is important to remember that this approximation starts to fail when $\beta \rightarrow 1$, which occurs at $Z \rightarrow 0$.

4 The Limiting Angular Velocity

To understand the origin of a maximal angular velocity it is instructive to look at the generic behavior of the function f . As already briefly mentioned, the latter will have two zeros on the positive axis and a local maximum between them. Obviously, the case where the local maximum falls below zero is a limiting case corresponding mathematically to $D = 0$ or alternatively to $r_1 = r_2$ (or in a yet different method setting $\alpha = 1$ (eq. 20) and physically corresponding to a maximally allowed angular velocity). The cusps [31] of the curves in figures (2a and 2b) display this behavior. After some algebra one obtains

$$\begin{aligned} \omega_{\text{max}}^0(Z) = \frac{c^3}{32GM} \left[\frac{5}{2} \sqrt{675 - 360(1 - Z^2) + 16(1 - Z^2)^2} \right. \\ \left. + (5 + 4(1 - Z^2))(45 + 4(1 - Z^2))^3 \right]^{1/2} : \quad (27) \end{aligned}$$

As described above, we can obtain the ‘absolute’ value of ω_{max} by setting $Z = 0$. This is the ‘absolute’ upper bound on the angular velocity which turns out to be

$$\omega_{\text{max}}^{0(1)} = \frac{5c^3}{32GM} : \quad (28)$$

A numerical value can be found by taking $M = 1.35M_\odot$, so that

$$\omega_{\text{max}}^0 = 2.35 \cdot 10^6 \text{ rad/s} \quad (29)$$

is only one order of magnitude away from the observed millisecond pulsars. When Z is different from zero, ω_{max} can be consistent with the largest angular velocities observed in millisecond pulsars [33]. The result for typical redshifts around $Z \approx 1$ is

$$\omega_{\text{max}}^0(Z) = \frac{c^3}{GM} \left[\frac{2}{3} (1 - Z) \right]^{3/2} \quad (30)$$

One can interpret the equation (30) in two different, but related ways. Both ways have to do with the evidence that millisecond pulsars are orthogonal rotators ($\alpha = \pi/2$) [9, 10, 11]. Since the right hand side of (30) agrees already with the angular velocity of fast spinning objects, the emission angle must be close to $\pi/2$ (see equation (14)). As we shall see below, this result can in turn be used to learn about the orientation of the magnetic axis in rapidly rotating objects, particularly neutron stars.

The standard model for the pulsar emission mechanism was developed independently by Pacini [36] and Gold [37] (see also ‘lighthouse’ model [38]), and will now be described briefly. Since the rotation axis is not aligned with the magnetic axis, a changing magnetic field will induce electric fields at the magnetic poles in for example, a neutron star. These electric fields will eject particles which will follow helicoidal paths around the magnetic field lines. The ejected particles will in turn, emit a narrow cone ($\approx 10^\circ$ [19]) of radiation parallel to the magnetic axis. From this argument it can be inferred that the angle between the magnetic axis and the rotation axis is approximately the same as the emission angle θ .

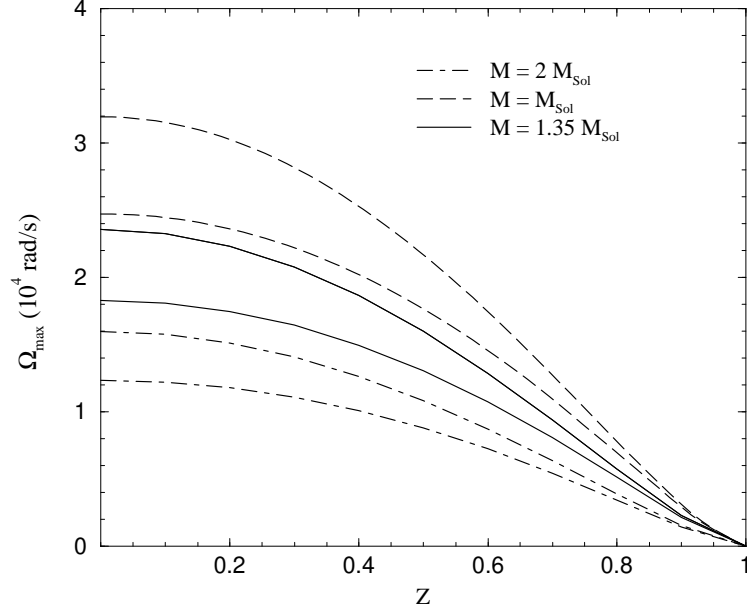


Figure 3: Maximum angular velocity as a function of the redshift for different masses. For each mass, there are two curves. The upper curve is the maximum angular velocity (Equation (27)) obtained from the perturbative metric. The lower curve for each mass corresponds to the analogous expression for the extended metric (33).

The emission angle has been measured indirectly from many pulsars by Kuzmin and Wu [9], and in their results, a strong correlation between orthogonal magnetic axes and fast millisecond pulsars is evident. This measured correlation agrees with our results and the results of [10, 11], which favor orthogonal rotators.

On the other hand, we can assume the theory outlined above to be valid, which allows us to determine Ω_{max} . Indeed, we can even assume that the angular velocity of fast rotating objects is close to the maximally allowed value. In other words we have Ω_{max} which essentially, knowing Ω_{max} , predicts the redshift. In turn, we can now extract the value of the radius. We will discuss this procedure taking realistic examples in the next section. Some examples of the behavior of Ω_{max}^0 as a function of the gravitational redshift are shown in Figure 3.

There has been a considerable amount of work done related to the maximum angular velocity. Haense et al. [13], Glendenning [39] and Koranda et al. [40] have used empirical formulae together with extensive numerical calculations to provide a lower bound for the period of rotation. Haense et al. [13] found the minimum period to be $T_{\text{min}} = 0.288 \text{ ms}$, assuming a mass of $1.44 M_{\text{Sol}}$. This period also depends on the minimum bound for the

redshift which was found to be $Z = 0.528$ [13]. If we use eq. (27) (in accordance with the evidence of milli-second pulsars being orthogonal rotators we use $\alpha = 2$) and the parameters just mentioned we obtain $T_{\text{min}} = 0.442 \text{ ms}$. However, if we use our absolute bound (eq. (28)) and the mass assumed by Haensel we obtain the very close value of $T_{\text{min}} = 0.284 \text{ ms}$. This is just a difference of just 1.4% which is rather gratifying recalling that our result has been obtained analytically by methods different from [13].

Other relevant work has been done related to the "mass-shedding limit" ([12], [41], [42]). This limit is conceptually different from what we have found and corresponds to the limit at which the neutron star would break apart. Lattimer and Prakash find for this limit

$$\omega_{\text{max}}^{(2)}(R) = 1045 \left(\frac{M}{M_\odot} \right)^{1/2} (10 \text{ km} / R)^{2/3} \text{ Hz}; \quad (31)$$

which is independent of the equation of state [17] and applicable for masses not very close the maximum mass. Equation (31) can be used for example, to find a limiting radius having an assumed or measured mass. While applying our results to find a radius we will compare our findings to the results when our maximal angular velocity is replaced by the one above. Here we note that that it is not straightforward to compare the radius independent limit (28) with (31) as the latter depends explicitly on R . However, it is obvious that both are of the same order of magnitude.

The orders of magnitude reached by the maximum angular velocity are quite large, but still less than the condition for slow rotation given by Zeldovich and Novikov [27]; even for the absolute maximum (Equation (28)). The condition for slow rotation ($J < M R_g c$) gives

$$\omega_{\text{max}}^{(3)} = \frac{5GM}{R^2 c} \quad (32)$$

which is one order of magnitude larger than our maximum upper bound when we take $R = R_g$, and even larger when we compare with the non-zero redshift case. Still, because our maximum angular velocity is comparable to the Zeldovich-Novikov condition, especially with $R > R_g$, we will make a better approximation for the metric in the following section.

5 Improvements: Extended Metric

Even though the perturbative metric (10) gives relevant results, a better approximation for the metric is given for instance in [43]. Assuming a negligible quadrupole moment, the second approximation the metric is

$$g_{tt} = 1 - \frac{2GM}{c^2 R} + \frac{1}{6} \frac{GM}{c^2 R}^3 - O \left(\frac{GM}{c^2 R}^4 \right) \quad (33)$$

$$g_t = \frac{J \sin^2(\theta)}{c^2 M} - \frac{2GM}{c^2 R} + 4 \frac{GM}{c^2 R}^2 + \frac{GM}{c^2 R}^3 + O \left(\frac{GM}{c^2 R}^4 \right) \quad (34)$$

$$g_{\theta\theta} = \frac{R^2 \sin^2(\theta)}{c^2} \left(1 + \frac{2GM}{c^2 R} + \frac{1}{2} \frac{GM}{c^2 R}^2 + O \left(\frac{GM}{c^2 R}^3 \right) \right)$$

One can apply the very same procedure as before. The resulting polynomial to be solved to obtain the two solutions for the radius is of fifth order in R . In consequence we can present the solution only numerically. An inspection of figures 2 and 3 shown that the new results, differ from the previous one only at very high angular velocities. The maximum angular velocity obtained using the extended metric is slightly higher than the one obtained analytically, so that eq. (27) for the maximum angular velocity is still a valid bound. However, in comparison to the first order metric we used before, it becomes clear that the limit on the maximal angular velocity improves, especially for the absolute limit at zero gravitational redshift.

6 Applications

Here we shall apply our results to some known compact objects such as Sirius B, an isolated neutron star, and several known pulsars.

Sirius B is the binary companion of the very bright Sirius A and is the closest White Dwarf to earth. Sirius B has been studied extensively, and the Gravitational Redshift has been measured accurately with the help of the Hubble space telescope [44]. Also, since it is a binary system, its mass has been measured accurately [45].

$$z = 0.999735 \pm 0.000015; M = 0.984M_{\odot} \quad (35)$$

According to eq. (27), we get a minimum period of

$$\frac{T_{\min}(\text{Sirius B})}{\sin} = 10.8 \text{ s} \quad (36)$$

This number does not change very much, had we applied the results from the extended metric.

The low mass X-Ray binary system EXO 0748-676 has been studied by Cottam et al. [46]. They managed to measure spectral absorption lines corresponding to a redshift of

$$z = 0.74 \quad (37)$$

This together with its mass (Assumed to be $1.35M_{\odot}$) gives

$$T_{\min}(\text{EXO 0748-676}) = 9.05 \cdot 10^4 \text{ s} \quad (38)$$

The value above has been obtained employing the extended metric (the corresponding value resulting from the first order approximation is $5.8 \cdot 10^4 \text{ s}$). The period for this neutron star has been measured to be $22 \cdot 10^3 \text{ s}$ [47], which is not too far away from the above limit given by T_{\min} . The predicted radius for the assumed mass and measured period and redshift, is 8.7 km .

In addition to the previous applications, our results concerning the maximum angular velocity, can be applied to millisecond pulsars. It is plausible to assume that for millisecond pulsars, the measured angular velocity is very close to the maximum angular velocity.

Pulsar	Period (m s)	M (M_{\odot})	Z	R (km)
P SR J1748-2446ad	1.396 [34]	1.35?	90?	0.834 20.1
P SR B1937+ 21	1.557 [35]	1.35?	90 [9]	0.836 20.2
P SR J1909-3744	2.95 [48]	1.438 [48]	90?	0.896 31.1
P SR 1855+ 09	5.3	1.35?	90 [9]	0.935 46.9
P SR J0737-3039 A	22.7 [49]	1.34 [49]	90?	0.976 133.6
P SR 0531+ 21	33.3	1.35?	90 [9]	0.982 164.4
P SR B1534+ 12	37.9 [50]	1.34 [50]	90?	0.983 165.9

Figure 4: Predicted Maximum Z and radius for several pulsars.

With this in mind, it is possible to predict a value for Z using equation (30), and a unique value for the radius using (17) or (18). Since $_{\text{max}}(Z)$ is a decreasing function, the predicted Z is actually a maximum bound, and if the "preferred" radius for the neutron star is r_2 , the predicted radius can be thought of as a maximum bound also. Here we present a table with predicted redshifts and radii for several fast millisecond pulsars.

From the table it can be inferred that for fast millisecond pulsars the radii are consistent with standard neutron star models [19]. However, for the slower millisecond pulsars, the maximum radius is slightly greater than what is predicted by most neutron star models, which implies that these neutron stars are probably not rotating exactly at their maximum angular velocity. In such a case the given radii should be interpreted as an upper bound which comes indeed close to the upper limit discussed in the introduction. Using equation (31) and assuming a mass of $1.4M_{\odot}$ the corresponding radius for P SR B1937+ 21 turns out to be 15.5 km [17], 5 km less than our result. For the slower millisecond pulsars, our results also predict slightly larger radii than those obtained by equation (31).

7 Conclusions

We have shown that the gravitational redshift in conjunction with global results from theoretical models can yield valuable information on the properties of rotating compact objects. Even though the determination of the radius in the presence of rotation is not a unique prescription, for relatively small angular velocities we can always opt for the lower result of the radius determination. With increasing angular velocity, a narrow range of possible radii can be defined. Alternatively, assuming that the angular velocity of the fast spinning neutron stars is close to its maximal value, we can either obtain a unique radius or an upper bound. The maximal angular velocity derived in text does not depend on the radius directly, but on the redshift which makes direct contact with existing or future observations. The absolute limit on (29) does not even depend on the redshift. It is satisfying that both these bounds come close to the observed values for millisecond pulsars. This implies that nature reaches here its maximally possible value. Another advantage of our approach is the confirmation of the emission angle of radiation in fast rotating neutron stars. The application of our results to existing objects clearly show that the method of

using the gravitational redshift for rotating objects is effective.

The important feature we would like to emphasize here is that we relate properties of Rotating Compact Objects to measurable quantities such as the Gravitational Redshift and the angular velocity. This way, our approach is semi-empirical and independent of model details.

As discussed in section four, our analytical findings regarding the maximal angular velocity agree with results obtained after numerical calculations. In this way, both, the analytical and numerical approach, corroborate each other.

Acknowledgment: We would like to thank Paolo Gondolo, from the University of Utah, for useful discussions and carefully reading the manuscript.

References

- [1] For a review see N. Stergioulas, *Living. Rev. Relativity*, 6, 3 (2003).
- [2] J. L. Friedman, in *"Millisecond Pulsars; A decade of Surprise"*, ASP Conference Series, 72, 177 (1995), A. S. Fruchter, M. Tavanian and D. C. Becker, eds.
- [3] W. Becker and G. Pavlov, *astro-ph/0208356*.
- [4] G. G. Pavlov and V. E. Zavlin in *Proceedings 21st Texas Symposium on Relativistic Astrophysics*, edited by R. Bandiera, R. M. Aiello and F. M. Annucci, World Scientific 2003, *arXiv:astro-ph/0305435*.
- [5] P. C. Vadya, *Proc. Indian. Acad. Sci., A* 33, 264 (1951)
- [6] V. S. Manko, E. W. Mielke and J. D. Sanabria-Gomez, *Physical Review D* 61, 081501 (2000).
- [7] L. A. Pachon, J. A. Rueda, J. D. Sanabria-Gomez, *Physical Review D* 73, 104038 (2006).
- [8] F. E. Schunck and E. W. Mielke, *Class. Quant. Grav.*, 20, R301, (2003); F. E. Schunck and A. R. Liddle, *Phys. Lett.* 404, 25 (1997).
- [9] A. D. Kuzmin and X. J. Wu, *Astrophysics and Space Science*. 190, 209-218 (1992).
- [10] K. Chen, M. Ruderman, T. Zhu, *Astrophysical Journal*. 493, 397403, (1998).
- [11] D. C. Backer, *Astrophys. Journal*, 493, 873-878, (1998).
- [12] J. M. Lattimer, M. Prakash, D. Masak and A. Yahil, *Astrophysical Journal*. 304, 241 (1990).
- [13] P. Haensel, J. P. Lasota and J. L. Zdunik, *Astronomy and Astrophysics*, 344, 151-153 (1999).
- [14] G. Baym, F. K. Lamb, *Encyclopedia of Physics* 1721-1725 (2005).

- [15] J. R. Oppenheimer and G. M. Volkov, *Phys. Rev.* 55, 374 (1939).
- [16] W. Baade, F. Zwicky, 1934. *Physical Review* . 45, 138, (1934).
- [17] J. M. Lattimer and M. Prakash, *Science*. 304, 536–542 (2004), astro-ph/0405262.
- [18] C. E. Rhoades and R. Ruini, *Physical Review Letters*. 32, 324 (1974).
- [19] S. L. Shapiro and S. A. Teukolsky. \The Physics of Compact Objects". John Wiley & sons (1983).
- [20] S. E. Thorsett and D. Chakrabarty, *Astrophysical Journal* 512, 288 (1999), astro-ph/9803260.
- [21] S. M. Carroll. \Spacetime and Geometry". Pearson Addison Wesley (2004).
- [22] This redshift factor is often denoted as $(1 + Z)^{-1}$ instead of just Z . This expression was first obtained by Luminet [23] in a different context.
- [23] J. P. Luminet, *Astronomy & Astrophysics*. 75, 228 (1979).
- [24] Even the gravitational redshift of the sun has been measured ([25], [26]).
- [25] T. P. Krisher, D. Morabito and J. D. Anderson, *Physical Review Letters*. 70, 2213 (1993).
- [26] J. L. Snider, *Physical Review Letters*. 28, 853 (1972).
- [27] Y. B. Zeldovich and I. D. Novikov. \Stars and Relativity". Dover (1971).
- [28] Angular momentum has a problem of factor 2 in General Relativity, see for instance R. W. Wald, \General Relativity", University of Chicago Press (1984) and E. W. Mielke, *Phys. Rev. D* 63, 044018 (2001) and references therein.
- [29] G. B. Cook, S. L. Shapiro and S. Teukolsky, *Astrophysical Journal*. 424, 823–845 (1994).
- [30] I. N. Bronstein and K. A. Semendjajew, \Handbook of Mathematics", Springer, Berlin (2004).
- [31] We use the word 'cusp' freely for the point where r_1 meets r_2 . This should not be confused with a cusp definition in catastrophe theory, see e.g. F. V. Kusmartsev, et al., *Phys. Lett. A* 157, 465 (1991).
- [32] Terms of order $(GM/c^3)^2$ and $(GM/c^3)^3$.
- [33] The highest observed spin rate is 716 Hz [34], $T = 1.5 \times 10^{-3}$ s.
- [34] J. W. T. Hessels, S. M. Ransom, I. H. Stairs, P. C. C. Freire, V. M. Kaspi, F. Camilo, *Science* 311 1901–190431 (2006).
- [35] M. Ashworth, A. G. Lyne and F. G. Smith, *Nature* 301, 313 (1983).

- [36] F. Pacini, *Nature*. 219, 145-146, (1968).
- [37] T. Gold, *Nature*. 221, 25-27, (1969).
- [38] D. R. Lorimer, *Living. Rev. Relativity*, 4, (2001), 5.
- [39] N. K. Glendenning, *Phys. Rev. D* 46, 4161 (1992)
- [40] S. Koranda, N. Stergioulas, J. L. Friedman, *Astrophysical Journal* 488, 799 (1997)
- [41] J. L. Friedman, L. Parker and J. R. Ipser, *Astrophysical Journal* 304, 115 (1986).
- [42] P. Haensel, M. Salgado and S. Bonazzola, *Astronomy & Astrophysics*. 296, 745 (1995).
- [43] E. M. Butterworth and J. R. Ipser, *Astrophysical Journal* 204, 200-223 (1976).
- [44] M. A. Barstow, M. R. Burleigh, J. B. Holberg, I. Hubeny, H. E. Bond and D. Koester, 4th European Workshop on White Dwarfs, *ASP Conference Series*. 334 (2005).
- [45] J. B. Holberg, M. A. Barstow and F. C. Bruhweiler, *Astrophysical Journal* 497, 935-942, (1998).
- [46] J. Cottam, F. Paerels & M. Mendez, *Nature* 420, 5154 (2002).
- [47] A. R. Villarreal and T. E. Strohmayer, *Astrophysical Journal* 614, (2004)
- [48] B. A. Jacoby, M. Bailes, M. H. van Kerkwijk, S. Ord, A. Hotan, S. R. Kulkarni, S. B. Anderson, *Astrophysical Journal* 599, L99-L102 (2003).
- [49] A. G. Lyne, M. Burgay and M. Kramer, *Science*. 303, 1153 (2004)
- [50] I. H. Stairs, Z. Arzoumanian, F. Camilo, A. G. Lyne, D. J. Nice, J. H. Taylor, S. E. Thorsett and A. Wolszczan. *Astrophysical Journal*, 505, 352 (1998).